Self-shielding of a plasma-exposed surface during extreme transient heat loads

J.J. Zielinski,[1] H.J. van der Meiden,[1] T.W. Morgan,[1] M.H.J. 't Hoen,[1] D.C. Schram,[2] and G. De Temmerman[1, a)]
[1)] *FOM Institute DIFFER, Ducth Institute For Fundamental Energy Research, Association EURATOM-FOM, Trilateral Euregio Cluster, P.O. Box 1207, 3430 BE Nieuwegein, The Netherlands*
[2)] *Department of Applied Physics, Eindhoven University of Technology, P.O. Box 513, 5600 MB Eindhoven, The Netherlands*

(Dated: 11 March 2014; Revised 11 March 2014)

The power deposition on a tungsten surface exposed to combined pulsed/continuous high power plasma is studied. A study of the correlation between the plasma parameters and the power deposition on the surface demonstrates the effect of particle recycling in the strongly-coupled regime. Upon increasing the input power to the plasma source, the energy density to the target firstly increases then decreases. We suggest that the sudden outgassing of hydrogen particles from the target and their subsequent ionization causes this. This back-flow of neutrals impedes the power transfer to the target, providing a shielding of the metal surface from the intense plasma flux.

The intense and localized transient heat and energy deposition during so-called Edge-Localized Modes (ELMs) are a major concern for the lifetime of the divertor materials in ITER[1] and future fusion devices. Numerous studies involving plasma guns[2], and electron beam facilities[3] have been performed to characterize the damage mechanisms of materials exposed to ELM-like transient loads. The intense inter-ELM plasma is known to induce strong morphology changes[4,5] and initial experiments with combined transient heat loading and continuous plasma exposure of tungsten surfaces revealed the existence of synergistic effects land increased material damage during transients[6,7].

Plasma-conditions in the divertor of future fusion devices ($n_e \sim 10^{21} m^{-3}$, $T_e \leq 10\ eV$) are such that the plasma-surface system will enter the strongly coupled-regime[8] i.e. that the mean free-path of the particles released from the surface is smaller than the characteristic plasma size, effectively trapping them in the near-surface region. Under those conditions, any change in the dynamic loading of the surface (e.g. during a transient event) might affect the near-surface plasma itself. This paper demonstrates that particle release from the surface caused by the rapid heating during ELM-like events can significantly cool-down the near-surface plasma effectively shielding the metal surface from plasma impact.

Experiments were performed in the Pilot-PSI linear plasma device[7]. The plasma is generated by a cascaded arc source and confined by a strong magnetic field (0.4 – 1.6 T). The continuous plasma can be combined with a transient heat and particle pulse (up to 1.2 GW·m^{-2} for 1.2 ms) , by superimposing a high current pulse onto the DC current, allowing the study of ELM effects on plasma-exposed surfaces[9,10].

In the present work the DC arc current was 200 A while the pulse current was varied up to 10 kA. The typical evolution of the discharge current during a pulse is shown in fig. 1. All experiments were performed using a hydrogen flow rate of 10 slm (1slm=4.4 × 10^{20} particles/s) and a magnetic field of 1.6 T. Samples were made of mirror-polished polycrystalline tungsten, ultrasonically cleaned in acetone and alcohol, and finally outgassed at 1000°C for 15 min.

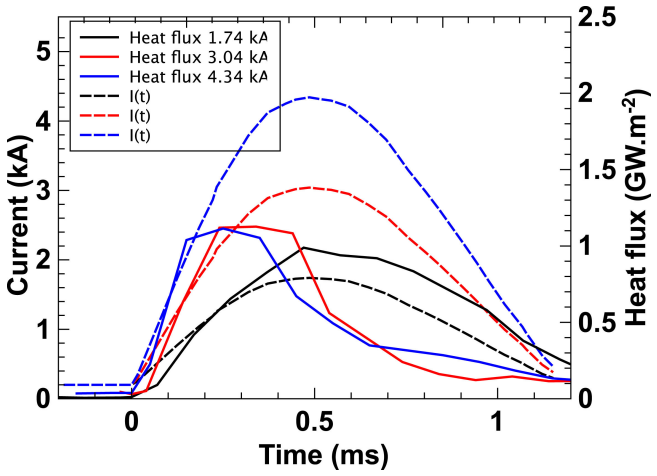

FIG. 1. Temporal variation of the maximum surface heat flux for different discharge currents. Also shown, is the temporal evolution of the discharge current during a plasma pulse.

An optical fiber-based timing system controls the discharge of the capacitor bank and synchronizes the different diagnostics. Radial profiles of electron temperature (T_e) and density (n_e) are obtained using single-pulse Thomson Scattering (TS)[11], either at 5 cm from the plasma source exit or 17 mm from the exposed surface (source-target distance is 54 cm). The TS system is set to measure at the peak of the discharge current during the pulse.

The surface temperature is monitored by a fast infrared camera (FLIR SC7500MB) in the wave-length

[a)] Electronic mail: g.c.detemmerman@differ.nl

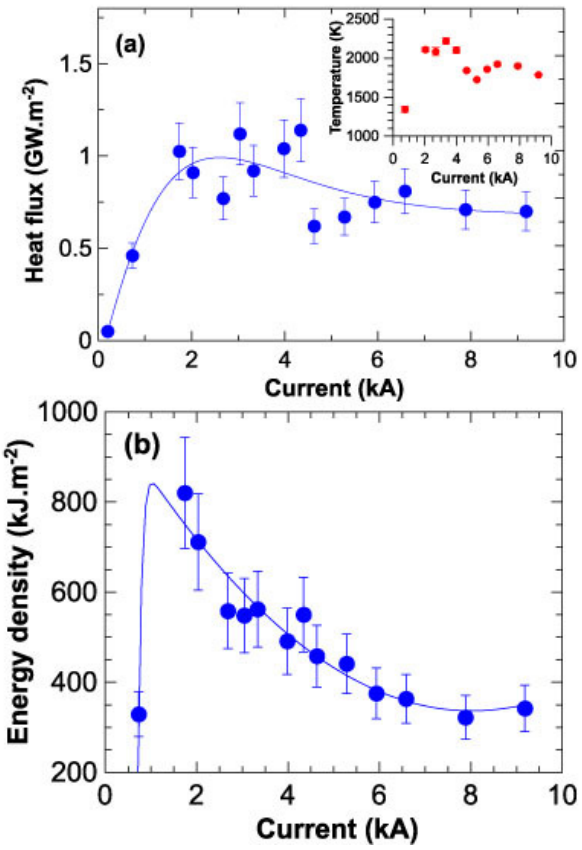

FIG. 2. Evolution of the (a) peak heat flux (b) energy density to the surface as a function of the discharge current. (b) is the temporal integration of (a). Solid lines are guide to the eye. The inset of (a) shows the maximum surface temperature during the pulse.

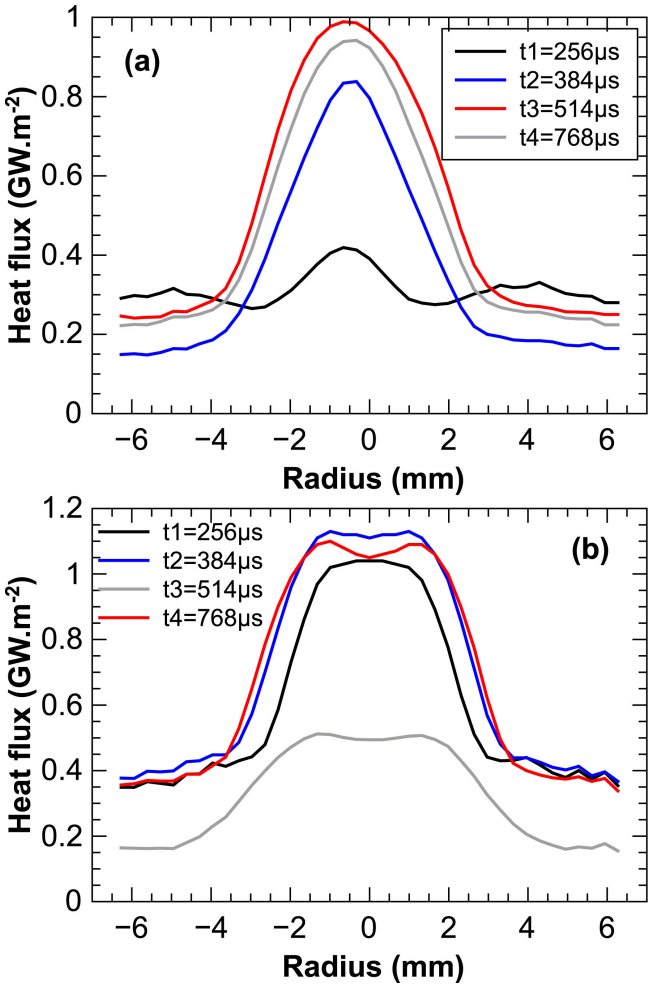

FIG. 3. Heat flux profile, as measured by infrared thermography, at different times (denoted in fig. 1 during the pulsed plasma for the cases I=1.74 kA (a) and (b) I=4.3 kA.

range 1.5-5.1 μm, operated at 7800 fps. The camera is calibrated up to 3300 K using a blackbody source. The temperature-dependence of the surface emissivity is taken into account[12]. The steady state temperature at the beam centre is about 800 - 900 K and increases up to 2000°K during the pulse. The temporal evolution of the surface temperature profile is used to calculate the plasma-deposited heat flux, using the THEODOR code[13].

Fig. 1 clearly shows a strong difference in time dependence of the heat flux when the source current maximum is varied from 1.74 to 4.34 kA. At the lowest value, the heat flow (and surface temperature) gradually increases with increasing current and is maximum roughly at the current maximum. However at higher peak source current, the behavior is totally different: first there is an initial rise of heat flow with rising current. But then at 2 kA the heat flow reaches a maximum with values around 1 GW$\cdot m^{-2}$ and a surface temperature of about 2000 K and then decreases abruptly. This maximum heat flow is reached earlier and earlier in the pulse: 200 μs to 100 μs from 3 to 4.3 kA respectively. This maximum heat flow is reached at an actual current around 2 kA, independent of the set current maximum.

Fig. 2 shows the variation of the peak heat flux on the target as a function of the maximum discharge current (i.e. peak input power). Being maximum around 2 kA, the heat flux first remains almost constant, despite the still increasing current and input power. The corresponding maximum surface temperature is about 2000 K (inset of 2). As shown in fig. 2, the peak energy density (corresponding to the peak heat flux in the middle of the plasma beam) varies from 0.3MJ$\cdot$m^{-2} at 0.7 kA to 0.8 MJ$\cdot$m^{-2} at 2 kA. Then, the peak energy density then monotonically decreases with increasing input power, down to 0.3 MJ$\cdot$m^{-2} at 9.2 kA. The heat flux risetime decreases with the peak current: from 500 μs at 1.7 kA to 200 and 120 μs at 3 and 4.3 kA. Also, the decay time becomes shorter. It is reduced from 600 μs at 1.74 to 350 μs at 4.34 kA. This apparent shortening of the pulse accounts for the decrease in the energy density. It is remarkable that the peak heat flux saturates

for current higher than 2 kA and decays after this value is reached, indicating that there is a screening of the surface by changes in the surface bordering plasma triggered by reaching the first time 2000 K. We will see later that also the H_α emission increases at that time and that a strong desorption of H atoms causes a temporary neutral gas cushion before the target.

The spatial profile of the heat flux is also modified when the current is increased above 1.7 kA. For a current of 1.7 kA (fig. 3 a), the heat flux profile remains Gaussian during the whole pulse. For higher discharge currents, a widening of the profile occurs and the profile even becomes hollow showing that the heat flux is suddenly reduced in the middle of the plasma beam (fig. 3 b). The TS measured density and temperature profile however remains Gaussian in both cases again indicating changes occuring very close to the surface.

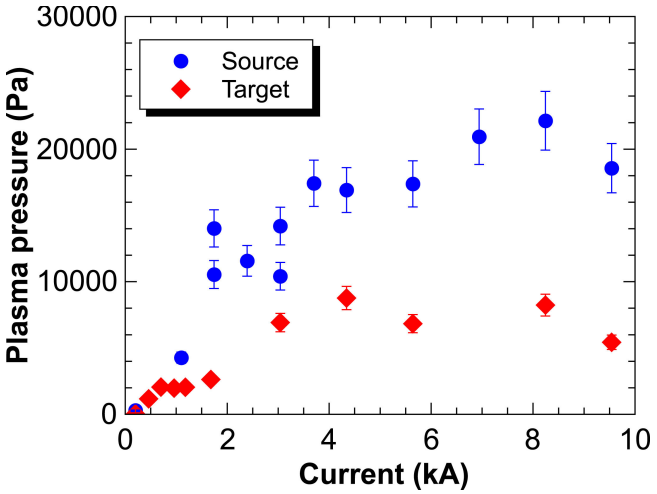

FIG. 4. Evolution of the plasma pressure close to the plasma source exit and close to the target surface as a function of the discharge current.

Fig. 4 shows the evolution of the plasma pressure (i.e. $n_e \times T_e$) in the beam centre measured at the time of the peak discharge current both close to the exit of the source and close to the plasma-exposed surface. Upstream, the plasma pressure increases strongly with discharge current up to 8 kA and tends to saturate for higher currents (fig. 4). The situation is very different close to the target (fig. 4). Firstly, the plasma pressure is lower at the target than upstream, which is linked to losses by recombination along the plasma beam. At currents below 3 kA, the evolution of the plasma pressure downstream and upstream both increase with discharge current. For higher currents however, the plasma pressure downstream saturates. The electron temperature decreases with increasing current from its maximum of 12 eV down to about 4 eV at 9.5 kA. At the same time, a doubling of the electron density is measured as the current increases from 6 and 8 kA. Therefore, while the plasma production at the source increases with increasing input power, a strong cooling of the plasma beam occurs close to the target at high currents.

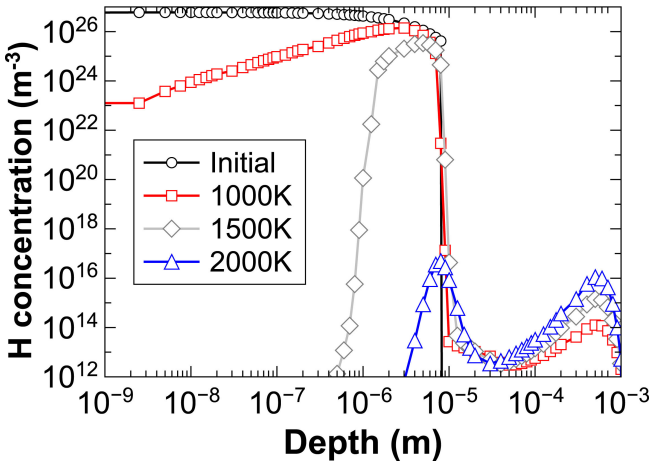

FIG. 5. Mobile deuterium concentration profile in tungsten, simulated by TMAP7, as a function of the peak temperature during a plasma pulse.

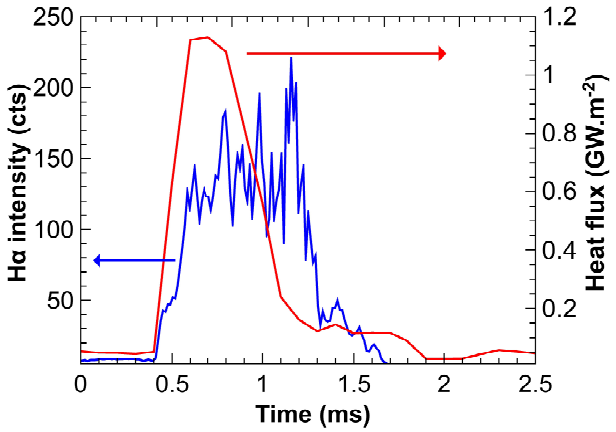

FIG. 6. Comparison of the temporal evolution of the peak heat flux and H_α emission from the surface.

Hydrogen is known to be retained in tungsten upon exposure to plasma[15]. Earlier dynamic studies[16,17], at much lower densities, indicate that during exposure the mobile hydrogen inventory is at least 2 times higher than the gas retention with plasma off, and increases linearly with the ion flux density (at least in the investigated flux range). The transient heat flux during a plasma pulse raises the surface temperature to about 2000 K on a sub-millisecond timescale. To assess the gas release caused by such a temperature rise, the TMAP7 code was used. TMAP7 is a one-dimensional program that solves the diffusion equation for deuterium in materials[18]. The rise and decay time of the surface temperature were assumed to be 0.5 ms, and 3 peak temperatures were considered: 1000, 1500, 2000 K. The mobile H concentration was assumed to have an exponential decay up to 9 μm below the

surface and a characteristic decay length of 3 μm, and a maximum concentration of 1% of the lattice density. Fig. 5 shows the evolution of the mobile D concentration profile in the surface as a function of the peak temperature during the pulse. At a peak temperature of 1500 K, about 91% of the mobile deuterium is released while at 2000 K this number reaches effectively 100%. It is striking that this corresponds to the maximum temperature reached during those experiments for currents of about 2 kA after which the temperature does not increase further (inset of fig. 2a). This is therefore a strong indication of a pronounced H release during a plasma pulse. A more direct evidence is shown in fig. 6 which shows that the H_α emission follows the heat flux evolution until the heat flux maximum and remains high up to 0.3 ms after the heat flux starts decaying. For densities above $10^{21} m^{-3}$, the $H_{n=3}$ level is mainly depopulated by electron excitation upward. H_α emission is then independent of n_e and is (for $T_e \geq 3$ eV) roughly proportional to the H atom density in front of the surface.

The ime-dependent heat flow at the target is observed to reach a maximum around 1 GW$\cdot m^{-2}$, when the current reaches around 2 kA. Then a sudden H atom release causes the heat flow to stop rising and to decrease despite the still increasing heat flow in the plasma from the source. We conclude that the sudden desorption of the dynamic H atom loading, during DC and in the early phase of the pulse, causes a strong build up of H atoms close to the target in a thin boundary layer. The mean free path for ionization, by electron impact ionization, of these recycled particles is much smaller than the plasma beam diameter (0.2 - 4 mm)[14], so that most are ionized close to the target and then return with the ion flow to the surface where they neutralize. Hence they recycle several times until the energy is consumed and T_e close to the surface starts decreasing. Only on longer time scale are neutrals lost to outside the plasma beam. Hence this H atoms inventory before the surface screens the surface from the incoming energetic plasma beam by taking up the energy in being ionized and heated and being lost to the surface again in several recycling events. The plasma will then cool close to the surface and even detach. A back-of-envelope calculation assuming that within the first micrometer the mobile H content is 10% of the lattice density (which corresponds to three times the density assumed in TMAP7) and that the release occurs over 0.05 ms (the H_α emission saturates almost as soon as the heat flux reaches 1 GW$\cdot m^{-2}$), the power density which can be dissipated by the additional neutral influx into the plasma is about 0.6 GW$\cdot m^{-2}$, and this will occur as long as the recycing continues. The gas desorption caused by the sudden temperature increase can thus impede the power transfer to the surface and actively shields the surface from the plasma. The apparence of a hollow heat flux profile is also an indication of a local cooling. The effect of the target outgassing on the near-surface plasma was already observed in[9].

A somewhat similar effect, vapour shielding[19], was observed where strong material ablation/evaporation dissipates the incoming plasma power. In the present case however, this occurs solely by outgassing of the mobile D atoms from the near-surface, and is amplified because of the very short mean-free path of released particles characteristic of the strongly-coupled regime. While such an effect has so far never been observed in tokamaks, no current device produces sufficient plasma densities in the divertor to enter the strongly couped regime. This represents an important feature of the strongly coupled regime of plasma-surface interactions which could lead to improved mitigation of transient plasma damage to the surface.

[1] R.A. Pitts, A. Kukushkin, A. Loarte, M. Merola, C.E. Kessel, V. Komarov, and M. Shimada, Phys. Scr. T138 014001 (2009)

[2] N. Klimov, V. Podkovyrov, A. Zhitlukhin, D. Kovalenko, B. Bazylev, G. Janeschitz, I. Landman, S. Pestchanyi, G. Federici, A. Loarte et al, J. Nucl. Mater. 390-391 721 (2009)

[3] T. Hirai, G. Pintsuk, J. Linke, and M. Batilliot, J. Nucl. Mat. 390-391 p 751-754 (2009)

[4] K. Tokunaga, M.J. Baldwin, R.P. Doerner, N. Noda, Y. Kubota, N. Yoshida, T. Sogabe, T. Kato, and B. Schedler, J. Nucl. Mater. 337-339 887 (2005)

[5] G. De Temmerman, K. Bystrov, J.J. Zielinski, M. Balden, G. Matern, C. Arnas, and L. Marot, J. Vac. Sci. Tech A 30 041306 (2012)

[6] K.R. Umstadter, D.L. Rudakov, W. Wampler, J.G. Watkins, and C.P.C Wong, J. Nucl. Mater. 415 p s83 (2011)

[7] G. De Temmerman, J.J. Zielinski, S. van Diepen, and Marot, and M. Price, Nucl. Fusion 51 073008 (2011)

[8] A.W. Kleyn, N.J. Lopes Cardozo, and U. Samm, Phys. Chem. Chem. Physics, 8 1761 (2006)

[9] G. De Temmerman, J.J. Zielinski, H. van der Meiden, W. Melissen, and J. Rapp, Appl. Phys. Lett. 97 081502 (2010)

[10] J.J. Zielinski, H.J. van der Meiden, T.W. Morgan, D.C. Schram and G. De Temmerman, Plasma. Source Sci. Tech. 21 065003 (2012)

[11] H.J. van der Meiden, R.S. Al, C.J. Barth , A.J.H. Donne, R. Engeln, W.J. Goedheer, B. de Groot, A.W. Kleyn, W.R. Koppers, N.J. Lopes Cardozo et al, Rev. Sci. Instrum. 79 p 013505 (2008)

[12] S. Roberts Phys. Rev. 114 p 104-115 (1959)

[13] A. Herrmann, W. Junker, K. Gunther, S. Bosch, M. Kaufmann, J. Neuhauser, G. Pautasso, Th. Richter and T. Schneider, Plasma Phys. Control. Fusion vol. 37 p. 17 (1995)

[14] R.K. Janev, W.D. Langer, K. Evans, D.E. Post (1987) *Elementary Processes in Hydrogen-Helium Plasmas* (Springer-Verlag: Heidelberg)

[15] J. Roth, and K. Schmid, Phys. Scr. T145 014031 (2011)

[16] G.M. Wright, D.G. Whyte, B. Lipschultz, R,P. Doerner, and J.G. Kulpin Journal of Nuclear Materials vol. 363-365 977 (2007)

[17] M. Yamagiwa, Y. Nakamura, N. Matsunami, N. Ohno, S. Kajita, M. Takagi, M. Tokitani, S. Masuzaki, A. Sagara and K. Nishimura, Phys. Scr., T145 014032 (2011)

[18] G. R. Longhurst, TMAP7 User Manual, Tech. Rep. (INEEL/EXT-04-02352 (Idaho: Idaho National Engineering and Environmental Laboratory), 2004).

[19] A. Hassanein, T. Sizyuk and I. Konkashbaev, J. Nucl. Mater., 390-391 (2009)